

Topology of optical vortex lines formed by the interference of three, four, and five plane waves

Kevin O'Holleran and Miles J. Padgett

Department of Physics and Astronomy, Kelvin Building, University of Glasgow, Glasgow, G12 8QQ, UK
k.oholleran@physics.gla.ac.uk

Mark R. Dennis

School of Mathematics, University of Southampton, Highfield, Southampton, SO17 1BJ, UK
Mark.Dennis@soton.ac.uk

Abstract: When three or more plane waves overlap in space, complete destructive interference occurs on nodal lines, also called phase singularities or optical vortices. For super positions of three plane waves, the vortices are straight, parallel lines. For four plane waves the vortices form an array of closed or open loops. For five or more plane waves the loops are irregular. We illustrate these patterns numerically and experimentally and explain the three-, four- and five-wave topologies with a phasor argument.

©2006 Optical Society of America

OCIS codes: (230.6120) Spatial light modulators; (260.2110) Electromagnetic theory; (999.9999) Optical vortices

References and links

1. J. F. Nye and M. V. Berry, "Dislocations in wave trains," *Proc. R. Soc. A* **336**, 165-90 (1974).
2. J. F. Nye, *Natural focusing and fine structure of light* (Institute of Physics Publishing, 1999).
3. M. V. Berry and M. R. Dennis, "Phase singularities in isotropic random waves," *Proc. R. Soc. A* **456**, 2059-79 (2000).
4. J. W. Goodman, *Statistical Optics* (Wiley, 1985).
5. D. Rozas, C. T. Law and G. A. Swartzlander, "Propagation dynamics of optical vortices," *J. Opt. Soc. Am. B* **14**, 3054-65 (1997).
6. M. V. Berry, "Much ado about nothing: optical dislocation lines (phase singularities, zeros, vortices)," in *Intl. Conf. on Singular Optics*, M. S. Soskin, ed., *Proc. SPIE* **3487**, 1-15 (1998).
7. J. Masajada and B. Dubik, "Optical vortex generation by three plane wave interference," *Opt. Commun.* **198**, 21-27 (2001).
8. M. V. Berry and M. R. Dennis, "Knotted and linked phase singularities in monochromatic waves," *Proc. R. Soc. A* **457**, 2251-2263 (2001).
9. M. V. Berry and M. R. Dennis, "Knotting and unknotting of phase singularities: Helmholtz waves, paraxial waves and waves in 2+1 spacetime," *J. Phys. A: Math. Gen.* **34**, 8877-88 (2001).
10. J. Leach, M. R. Dennis, J. Courtial and M. J. Padgett, "Knotted threads of darkness," *Nature* **432**, 165 (2004).
11. J. Leach, M. R. Dennis, J. Courtial and M. J. Padgett, "Vortex knots in light," *New J. Phys.* **7**, 55 (2005).
12. M. V. Berry, J. F. Nye and F. J. Wright, "The elliptic umbilic diffraction catastrophe," *Phil. Trans. R. Soc. A* **291**, 453-84 (1979).
13. E. Schonbrun, R. Piestun, P. Jordan, J. Cooper, K. D. Wulff, J. Courtial, and M. Padgett, "3D interferometric optical tweezers using a single spatial light modulator," *Opt. Express* **13**, 3777-3786 (2005).
14. W. H. F. Talbot, "Facts relating to optical science, No. IV," *London Edinburgh Dublin Philos. Mag. J. Sci.* **9**, 401-407 (1836).
15. K. Patorski, "The self-imaging phenomenon and its applications," *Progress in Optics* **XXVII**, 103-108 (1989).
16. J. F. Nye, "Local solutions for the interaction of wave dislocations," *J. Opt. A: Pure Appl. Opt.* **6**, S251-S254 (2004).
17. J. F. Nye, "Dislocation lines in the hyperbolic umbilic diffraction catastrophe," *Proc. R. Soc. A*, in press (2006).
18. M. R. Dennis, "Local phase structure of wave dislocation lines: twist and twirl," *J. Opt. A: Pure Appl. Opt.* **6**, S202-S208 (2004).

1. Introduction

A feature of wave superposition is that one plus one does not necessarily equal two: the interference of two equivalent waves can result in zero. In general, when three or more scalar waves interfere in space, complete destructive interference occurs on lines, called nodal lines, phase singularities, wave dislocations or optical vortices [1], studied in singular optics [2]. The singular nature of nodes arises since when the complex number describing the wave is zero, the argument is not defined (singular), and nearby all phases between 0 and 2π occur, increasing in either a clockwise or counterclockwise sense (Fig. 1).

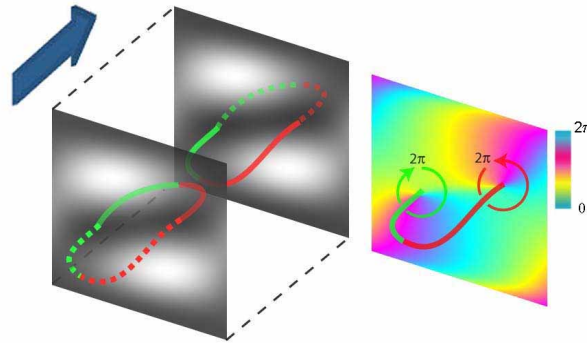


Fig. 1. Optical vortex line in an interference field. Left: periodic cell containing a vortex loop (dotted lines are parts of the loop outside the primitive cell). The intensity on the front and back planes is also represented. Right: phase cross section of the front/back face of the cell. The phase circulates in opposite directions at different points on the vortex line.

In a three-dimensional, random light field such as laser speckle, the nodal lines form a complicated tangle [3]. As with all optical fields, speckle patterns can be represented, through Fourier analysis, by a superposition of many plane waves with different directions and phases [4]. The connection between optical vortices in 3D and the plane wave decomposition is complicated as the position of nodes depends nonlinearly on the amplitudes and directions of the plane waves. Our aim here is to understand this connection for a small number of waves, namely superpositions of three, four and five plane waves.

Experimentally, vortex line geometry can be determined by imaging the intensity and phase distribution in successive beam cross-sections, within which the vortices are dark points. Identification of these points in successive cross-sections allows the complete 3D structure to be deduced. This approach complements the dynamical picture of optical vortices [5], in which propagation is associated with evolution of the two-dimensional pattern. Thus, in two dimensions, the creation or annihilation of a pair of oppositely signed vortices is equivalent to nodal line 'hairpins' [6] (Fig. 1). The apparent change in handedness occurring at the extremes of such a hairpin arises from its definition with respect to the propagation direction. The sense of phase circulation around the vortex line, and hence energy flow, is preserved at all points around the loop [6].

In an interference pattern made by superposing three plane waves, the vortex lines are straight and parallel, so in a cross-section, there is a regular array of vortex points [7]. In this paper we consider both more plane waves and most importantly, three spatial dimensions. In general, for four or more plane waves, the vortex lines are curved, typically forming closed loops. In special cases, vortex lines can form unusual topologies, such as links or knots (examples of which were proposed in Bessel beams [8, 9] and experimentally realized with Laguerre-Gauss beams [10, 11]). The present work is also related to phase singularities in the canonical three-dimensional diffraction catastrophes [12], whose complicated structure can be approximated using the superposition of a small number of plane waves.

The simple plane wave combinations we describe here are synthesized experimentally using a spatial light modulator (SLM) as a hologram. We address the SLM to produce a k -space distribution of paraxial plane waves [13]. The plane of the SLM is imaged to a CCD detector where the interference patterns are recorded. Our experimental setup is similar to that described in Ref. [11], except that the CCD is mounted on a motorized stage enabling a succession of images corresponding to neighboring cross-section to be obtained. Extending the setup so that the SLM is in one arm of an interferometer allows the phase structure to be recorded. We experimentally determine the vortex positions primarily using intensity measurements but confirm with reference to the phase measurements (as in Fig. 4 later).

2. Numerical calculations of vortex topology

Numerical characterization of the vortex topology in an arbitrarily large, finite interference pattern is problematic since ambiguities arise where vortex lines meet the volume edge. We overcome this problem by restricting the wave vectors to lie on a regular, rectangular grid in k -space, with spacing Δk . This results in an interference pattern that is periodic both transversally and axially (the Talbot effect [14, 15]), with repeat periods of $2\pi/\Delta k$ and $4\pi k_0/\Delta k^2$ respectively. This ‘Talbot cell’ can be tiled to give the interference pattern, and therefore the vortex structure, over all space (Figs. 1, 2, and 3) without ambiguity.

The location of a vortex within a cross-section is found by examining the phase structure around each pixel, a change of $\pm 2\pi$ indicating a vortex. Knowledge of whether two vortex points in neighboring planes form part of the same line is limited by the spatial resolution. However, since vortex lines are continuous, ambiguity only arises when two different lines approach (characteristically in an ‘avoided crossing’ or ‘reconnection’ [9, 16]). A vortex line, traced through the Talbot cell, can leave and re-enter at the associated point on the opposite face before arriving back at its starting position. Whether the vortex structure corresponds to a closed loop or open, infinite line is deduced from the number of cell crossings: a vortex line forms a closed loop if and only if the total signed cell crossing number is zero. The experimental correspond to the numerical simulations.

3. Phasor argument for vortex topology

The topological form of vortex lines resulting from the interference between N waves with wavevectors \mathbf{k}_n (for $n=1,\dots,N$) can be understood using phasors. At a particular position, the interference is calculated in the Argand plane by the vector addition of the individual phasors, ψ_n , of magnitude $a_n = |\psi_n|$ and argument $\arg \psi_n$, i.e. the total field at the point is $\sum_{n=1}^N \psi_n$. The waves are labeled in order of decreasing magnitude $a_1 \geq a_2 \geq \dots \geq a_N$.

At a vortex, the phasors form a closed loop. For a small number of interfering waves, the possible vortex topologies may be understood from the geometry of the phasor pattern. The simplest interference is between two waves, complete cancellation only occurring if the interfering waves have the same amplitude and opposite phase, $\psi_1 = -\psi_2$. This is a single real condition (i.e. has codimension one), and in three dimensions, occurs on surfaces.

Since labeling is in order of decreasing magnitude, for a superposition of three waves, cancellation can only occur if $a_1 \leq a_2 + a_3$, allowing a triangular configuration of the phasors. Under a different ordering of the phasors, the triangle may be reflected or rotated, but its shape cannot change. Along a vortex line, the phasor triangle rotates, so each component plane wave changes by the same phase, which can only be satisfied if the vortex direction is that in which the components of \mathbf{k}_n are the same. Therefore, the vortex structures arising from three plane waves are straight lines in the same direction, $\mathbf{k}_1 \times \mathbf{k}_2 + \mathbf{k}_2 \times \mathbf{k}_3 + \mathbf{k}_3 \times \mathbf{k}_1$, as in Fig. 2(a).

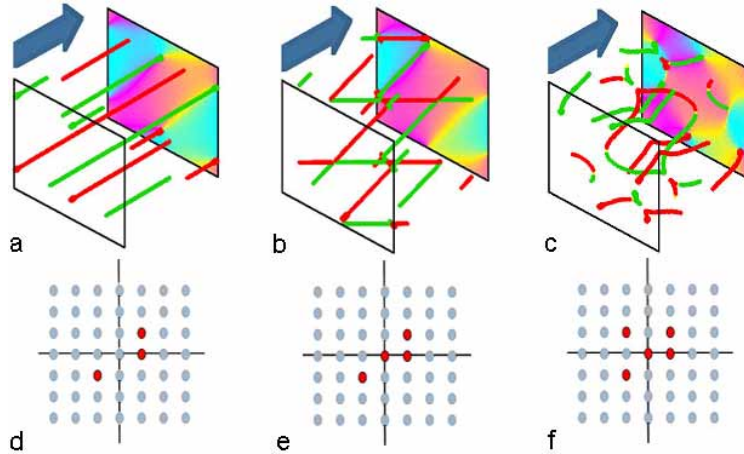


Fig. 2. Calculated vortex structure for three, four and five equal-amplitude plane waves (a, b, c) and their respective k -space configuration (d, e, f). Each is calculated on a $256 \times 256 \times 256$ Talbot cell.

For a superposition of four waves, cancellation can only occur if $a_1 \leq a_2 + a_3 + a_4$, giving a quadrilateral configuration of the phasors. With the magnitudes and wavevectors of the four waves fixed, the relative phases constitute three additional degrees of freedom. All possible phase relationships are explored throughout the three-dimensional Talbot cell. Consequently, a change to the initial phase of any of the superposed waves results only in a spatial translation, and does not affect any aspect of the vortex geometry.

When the four waves have the same magnitude, the closed loop of phasors forms a rhombus, where $\psi_1 = -\psi_3$ and $\psi_2 = -\psi_4$. The vortex follows the intersection of two planes, determined by the two-wave interference described above (for waves 1 and 3, and 2 and 4), and is therefore again a straight line. However, under different orderings, a rhombus is also possible if $\psi_1 = -\psi_2$ and $\psi_3 = -\psi_4$ or $\psi_1 = -\psi_4$ and $\psi_2 = -\psi_3$. Hence, there are three characteristic straight line vortex directions, along which the rhombus rotates and deforms. As the rhombus deforms, it may pass through a ‘flat’ configuration. At this point, the phasor pairs are identical, and the vortex lines cross [9, 16], as in Fig. 2(b).

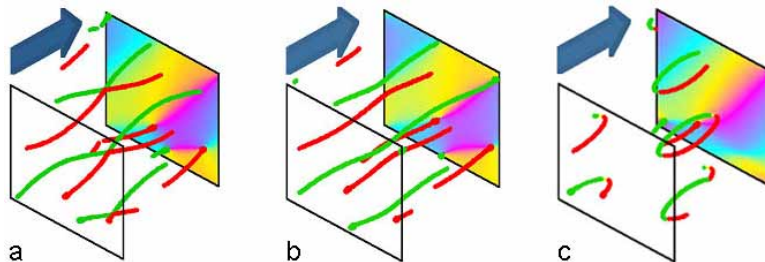


Fig. 3. The calculated vortex structures for four plane wave superpositions with amplitudes: a), $a_1 + a_4 = a_2 + a_3$ (b), $a_1 + a_4 < a_2 + a_3$ (c), $a_1 + a_4 > a_2 + a_3$. The choice of k -vectors is the same as Fig. 2 (b), given in Fig. 2 (e). Attached multimedia shows rotation of cells around the optical axes (a, b, c) (1.4Mb, 1.3Mb, 1.1Mb).

In four-wave interference patterns, the vortex behavior can be completely understood, the topology depending only on the relative magnitudes. These cases are illustrated in 3, and experimentally in Fig. 4. Most similar to the equal-amplitude case is when the amplitudes are not equal, but $a_1 + a_4 = a_2 + a_3$. The vortex lines are curved, but at particular points within the

Talbot cell the four phasors are co-linear. As with the equal magnitude case, this corresponds to a vortices crossing, as in Fig. 3(a). More generally, either $a_1 + a_4 < a_2 + a_3$ or $a_1 + a_4 > a_2 + a_3$. The former gives rise to an array of helical vortex lines (Fig. 3 (b), 4 (a)) whereas the latter gives an array of identical vortex loops [Figs. 3(c) and 4(b)], some of which may fall across the Talbot cell boundary. This difference is illustrated in Fig. 5, where phasor configurations along vortex lines in the two cases are shown. When $a_1 + a_4 > a_2 + a_3$ (loops) the smallest magnitude cannot execute a full 2π rotation about the largest; this geometric constraint limits the maximum phase difference between any two phasors and hence the spatial extent of the vortex line, which must therefore be a loop. By contrast, when $a_1 + a_4 < a_2 + a_3$ (lines) the relative phase difference between the smallest amplitude phasor and the remaining three can cycle unidirectionally through the full 2π range. In this case the vortex line can extend indefinitely (essentially a perturbed three wave superposition) [2].

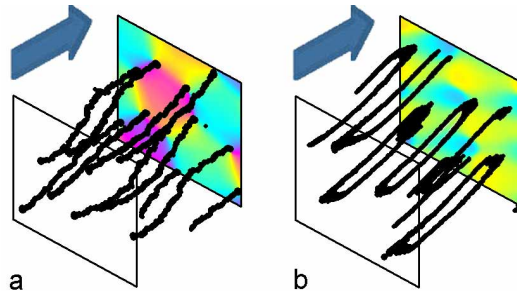


Fig. 4. Experimentally measured vortex structures from the superposition of 4 plane waves with amplitudes giving rise to a) twisted vortex lines and b) vortex loops. The choice of k -vectors differs slightly from that in Fig. 3(b) and Fig. 3(c). Attached multimedia shows rotation of each cell around the optical axis (1.9Mb, 1.8Mb).

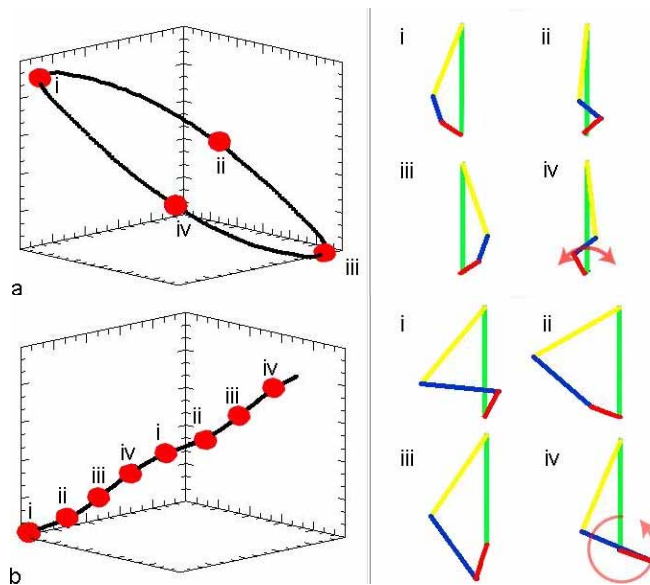


Fig. 5. Left: Vortex line in (x, y, z) . Right: phasor diagrams at the points highlighted on a vortex a) loop and b) a line. For clarity, the orientation of the largest magnitude phasor has been fixed. The red arrows show the angular range of the smallest phasor, with respect to the largest. Note that in (a) this is restricted to less than 2π . Attached multimedia shows phasor configuration changing as the vortex paths are followed (2.3Mb, 2.1Mb).

For interference between five waves, cancellation requires the phasors to lie on a pentagon (up to reordering), and the geometry of the curved vortex lines cannot be simply described. Figure 6 shows superpositions of the same five waves as Fig. 2(c) but with different choices of relative phases. There are four relative phases, so translation in three dimensions is insufficient to account for all possible phase relationships; the pattern is not specified uniquely by the magnitudes alone. This extends to arbitrary numbers of interfering waves, where optical vortex topology is generally complicated.

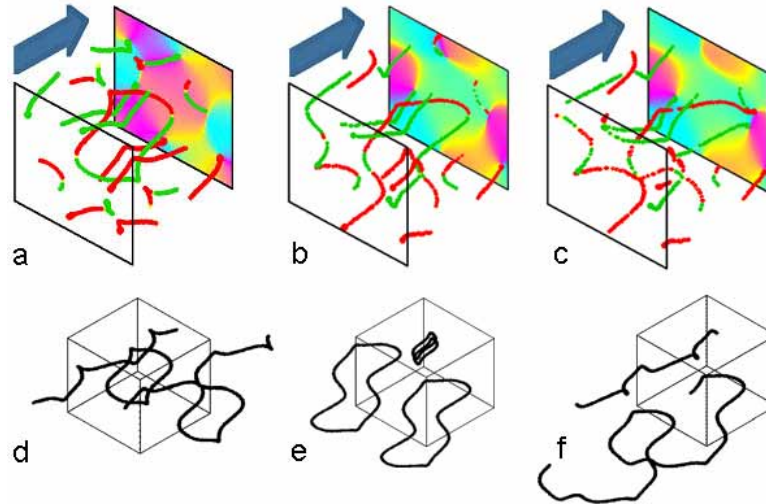


Fig. 6. Examples of different vortex topologies that can be obtained from five waves of the same magnitude but different relative phase. Fig. 6 (a) is the same Talbot cell as Fig. 2(c). Figs. 6(b) and 6(c) are Talbot cells from the same wave magnitudes as (a) but with one wave advanced in phase by $\pi/2$ and $\pi/3$. Figs. 6(d),6(e), and 6(f) are their unwrapped counterparts.

4. Discussion

We have explained the geometry of optical vortex lines in three-dimensional superpositions of small numbers of plane waves. Unlike superpositions of many plane waves, the topology of vortices in 3- and 4-wave superpositions is relatively restricted, and can be understood completely using phasor geometry. The characteristic tangle of vortex lines that is familiar for more general, many-wave superpositions begins for five waves. Some of the features described here occur in diffraction catastrophes [12], where certain domains can be asymptotically approximated by superpositions of a few plane waves. In particular, four-wave interference patterns occur in the hyperbolic umbilic diffraction catastrophe [17], which notably has a region in which phase singularities intersect and can be asymptotically approximated by a superposition of four plane waves of equal amplitude. It should be noted that, although our experiments and numerical illustrations require periodicity and paraxiality, the theoretical justification of these geometries using phasors do not, and apply for general superpositions of plane waves. The phasor methods we have employed here might prove useful more generally in the analysis of optical vortices, for instance, in describing the anisotropy of optical vortex cores [3], as well as how the curvature, phase structure and anisotropy changes along an optical vortex line [18].

Acknowledgments

The authors thank Professor Michael Berry and Dr. Sonja Franke-Arnold for useful discussions. This work is supported by the Leverhulme Trust and MRD acknowledges support from the Royal Society.